Ionophore A23187. Solution Conformations of the Calcium Complex and Free Acid Deduced from Proton and Carbon-13 Nuclear Magnetic Resonance Studies†

Charles M. Deber* and Douglas R. Pfeiffer

ABSTRACT: Proton and carbon-13 nuclear magnetic resonance (NMR) spectra have been used to deduce possible biologically relevant conformations of ionophore A23187 as the free acid, and as the calcium complex, in solution. By analysis of coupling constants and dihedral angles obtained from 270-MHz proton NMR, A23187 free acid molecules and individual A23187 anions which comprise the calcium complex are found to differ principally by the rotational state of a carbon–carbon single bond near the benzoxazole ring. Proton T_1 relaxation data and measurements of rotational correlation times confirm the dimeric nature of the calcium complex vs. the free acid monomer. Using the deduced pseudocyclic conformation for the A23187 anion, in conjunction with model-building studies, a conformation for the calcium complex is proposed, in which the benzoxazole carboxylate oxygen, the ketopyrrole oxygen, and the benzoxazole (ring) nitrogen atom of each molecule are the major participants in calcium binding. Additional stabilization of the structure is possible through the formation of a postulated hydrogen bond bridge between the pyrrole NH proton and benzoxazole carboxylate oxygen.

The naturally occurring ionophore A23187 is finding increasing use in cell physiological studies to investigate the mechanism of complex physiological processes. Examples of this work include studies of several types of secretion phenomena (Thoa et al., 1974; Prince et al., 1973; Grenier et al., 1974; Foreman et al., 1973; Holz, 1975; Wollheim et al., 1975), contraction (Schaffer et al., 1974; Schwartz et al., 1974; Levy et al., 1973; Schroeder and Strickland, 1974), parthenogenesis (Chambers et al., 1974; Steinhardt et al., 1974; Steinhardt and Epel, 1974), the effects of divalent cations on permeability properties of mitochondria and other membranous structures (Reed and Lardy, 1972a,b; Reed et al., 1975; Wong et al., 1973; Selinger et al., 1974), lymphocyte transformation (Luckasen et al., 1974; Maino et al., 1974), sperm motility (Reed and Lardy, 1972b), and gluconeogenesis (Zahlten et al., 1973). In many cases, the presence of A23187 and Ca^{2+} has been found to mimic the effects of hormones or nervous excitation which normally control these processes in vivo. The selectivity for divalent over monovalent cations displayed by this ionophore (Reed and Lardy, 1972a,b; Pfeiffer et al., 1974) has helped foster its wide use and the results obtained in these latter studies strengthen the concept that alteration in cellular Ca^{2+} levels or fluxes is an important component of cellular control mechanisms.

In contrast to this substantial literature on physiological effects of A23187, the chemistry of the compound has not yet been extensively studied. The chemical composition has been determined (see Figure 1) and the x-ray structure of the ionophore in the free acid form has been reported (Chaney et al., 1974). The free form, and some metal ion complexes, have been studied in solution by ultraviolet and fluorescence spectroscopy (Pfeiffer et al., 1974; Case et al., 1974; Reed et al., 1975; Caswell and Pressman, 1972), the Cu^{2+} and Mn^{2+} complexes have been studied by electron paramagnetic resonance (EPR) (Puskin and Gunter, 1975), and relative binding constants for several cations have been measured (Pfeiffer et al., 1974; Puskin and Gunter, 1975; Caswell and Pressman, 1972). Spectral observations in natural membranes (Caswell and Pressman, 1972; Case et al., 1974) and in phospholipid dispersions (Puskin and Gunter, 1975) are also consistent with the original hypothesis by Reed and Lardy (1972a) that A23187 catalyzes an electroneutral exchange of divalent metal ions for two protons through the formation of a charge-neutral lipid soluble complex. Since further knowledge of the chemical properties of A23187, including cation specificity and the mechanism by which Ca^{2+} and H^+ transport is mediated, would clearly aid in the evaluation and extension of physiological data, we have examined the solution conformation(s) of this antibiotic by proton and carbon-13 nuclear magnetic resonance (NMR) spectroscopy.

In distinction to the group of cyclic depsipeptides such as valinomycin and enniatin (Ovchinnikov et al., 1974) or cyclic peptides (Deber and Blout, 1974; Patel, 1973), A23187 may be placed among those ionophores (including X-537-A, nigericin, and monensin) which contain an ionizable carboxylic acid function. In fact, the simplest form of an A23187–calcium "complex" would be the calcium salt of an organic acid with the A23187 molecule serving as the "anion" (e.g., as in calcium acetate, $Ca(OAc)_2$). However, it appears widely accepted that the positively charged cation must be encased in the central cavity of the carrier molecule (Simon et al., 1973; Truter, 1973), surrounded by appropriately oriented groups of electronegative atoms which, in effect, replace the cation hydration shell (Eisenman and Krasne, 1973). Thus, any proposal for the membrane-active conformation of A23187 should consider not only the anticipated interaction of calcium with the carboxylate substituent (on the benzoxazole group), but any additional stabili-

† From the Institute for Enzyme Research, University of Wisconsin, Madison, Wisconsin 53706. *Received May 8, 1975.* This work was supported, in part, by the National Institutes of Health (Grant No. AM 10334) and by a grant (to C.M.D.) from the University of Wisconsin Research Committee.

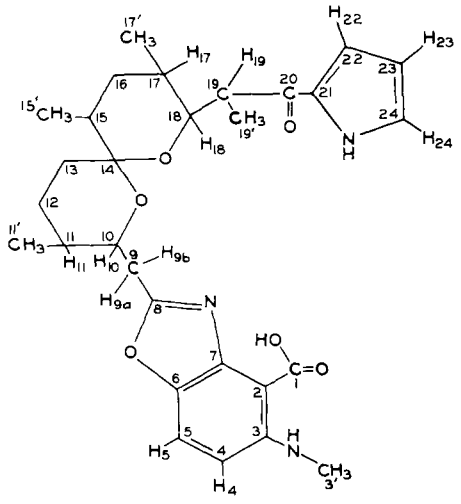

FIGURE 1: Structural formula of ionophore A23187. The numbering system follows that of Chaney et al. (1974). The benzoxazole portion of the molecule includes atoms from C_1 to C_8; the spiroketal portion, atoms C_{10} to C_{18}; and the ketopyrrole portion, atoms C_{20} to C_{24}. Stereochemistry not indicated.

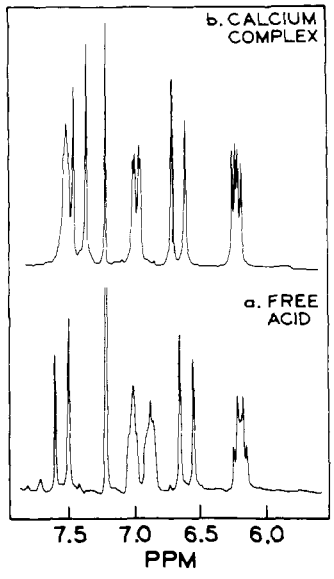

FIGURE 2: Proton NMR spectra (90 MHz) of the aromatic region of A23187; concentration, 10 mg/ml in $CDCl_3$. Chemical shifts given in parts per million downfield from internal tetramethylsilane (Me_4Si). The singlet near 7.25 ppm in each spectrum is residual $CHCl_3$. Spectra are: (a) free acid; (b) calcium complex. In b, N-H protons have been exchanged with deuterium.

zation and shielding of cation from solvent which may be obtained through further participation in binding of other functional groups in the molecule. Spectral data on A23187 quoted above have been considered consistent with these concepts. In the NMR data presented here, evidence emerges for a folded A23187 complex conformation, with the involvement of ligands at opposite ends of the molecule in calcium binding.

Materials and Methods

The antibiotic A23187, isolated from cultures of *Streptomyces chartreusensis*, was a gift from Dr. Robert Hamill of Eli Lilly and Co. NMR spectra were determined at probe temperatures on the Bruker HX-90E or the Bruker HX-270 spectrometers located in the School of Pharmacy and Department of Chemistry, University of Wisconsin, respectively. Deuterated solvents were purchased from Merck and Co.

Solutions of A23187 (15–20 m*M*) in chloroform-*d* were used in most NMR studies. The calcium complex was prepared by vortexing these solutions with an equal volume of aqueous calcium chloride ($CaCl_2$, 0.5 *M*) containing Tris base (0.1 *M*). Following centrifugation to separate the two phases, an aliquot of the organic phase was taken for examination by NMR. The preparation of a 2:1 A23187:Ca^{2+} complex by this technique (Reed and Lardy, 1972a; Pfeiffer et al., 1974; cf. Puskin and Gunter, 1975) was verified by Ca^{2+} analysis using atomic absorption spectroscopy. Evidence confirming that both ionophore carboxylic acid functions are deprotonated when the complex is prepared in this manner has recently been obtained in our laboratory (D. R. Pfeiffer and H. A. Lardy, manuscript in preparation).

Results

Proton NMR Spectra. A comparison of the proton NMR spectra (aromatic region) at 90 MHz of A23187 free acid and the calcium complex is shown in Figure 2. In accord with the assignments of Chaney et al. (1974), the AB quartet centered at 6.65 and 7.59 ppm in the acid spectrum is due to the two protonated positions on the benzoxazole ring (H_4 and H_5) (refer to Figure 1 for numbering), while the three multiplets at 6.24, 6.92, and 7.05 ppm correspond to

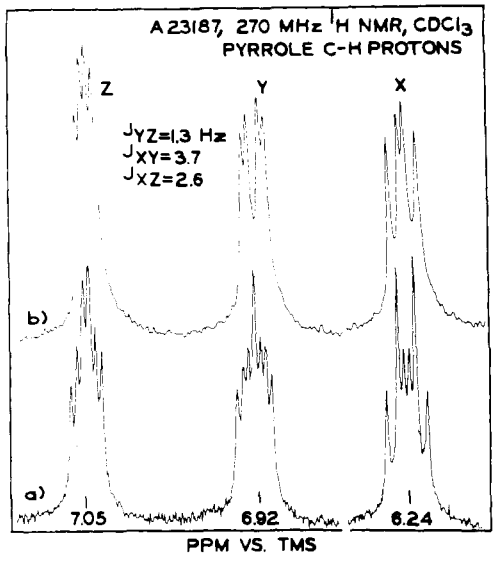

FIGURE 3: Proton NMR spectra (270 MHz) of the three pyrrole ring C-H protons of A23187 free acid on an expanded scale; concentration, 8 mg/ml in $CDCl_3$. Spectra are: (a) the fully coupled resonances and (b) the same spectrum but with homonuclear spin decoupling at the pyrrole N-H.

the three carbon-bound protons of the pyrrole moiety (H_{22}, H_{23}, and H_{24}). Upon complexing with calcium (Figure 2b), chemical-shift changes are observed in most of these resonances, most prominently in one pyrrole proton, which shifts at least 0.5-ppm downfield.

Within the two groupings of aromatic protons, some further assignments can be made. In the benzoxazole AB quartet, it is possible to assign the upfield half (centered at 6.65 ppm) to H_4 on the basis of a small, but perceptible long-range coupling of this resonance to its neighboring N-H proton. A more detailed analysis of the spectrum due to three pyrrole protons, performed at 270 MHz, is presented in Figure 3. Spectrum a shows the fully coupled patterns of

H_{22}, H_{23}, and H_{24} on an expanded scale, while b shows the effects on a due to homonuclear decoupling at the pyrrole N-H proton (at 9.70 ppm). All three patterns in b have been simplified, indicating that the N-H is coupled to all three ring protons. This simplification facilitated the complete determination of coupling constants arising between the ring protons; these values are shown in Figure 3. On the basis of the observations that (i) the proton resonating at 6.24 ppm is coupled with the two largest coupling constants (2.6 and 3.7 Hz) to the other two, suggesting it is most likely to be vicinal to both of them (i.e., it is located between the other two in the ring), and (ii) only one pyrrole proton is not adjacent either to an electronegative atom (nitrogen) or substituent (carbonyl), one may assign the highest field proton of the three to H_{23}. However, the determination as to which of the two lower field protons, separated by only 0.13 ppm, corresponds to either H_{22} or H_{24} remains problematical. In the model compound *N*-methylpyrrole-2-carboxaldehyde, the three resonances appear at 6.20, 6.97, and 7.12 and have coupling patterns formally analogous to those in Figure 3b; these resonances were assigned by Arlinger et al. (1970) to H_{23}, H_{22}, and H_{24}, respectively (using the A23187 numbering for the present comparison). Coupling of the aldehydic proton to the lowest field resonance was cited as one reason for the assignment of the downfield proton to H_{24}. In concert with this, D. F. Hillenbrand (University of Wisconsin, unpublished results) has achieved a computer-simulated match to the spectrum of the related nonmethylated model compound, pyrrole-2-carboxaldehyde. Resonance patterns, chemical shifts, and coupling constants are again similar to those discussed above, and nonzero coupling to the aldehydic proton (1.2 Hz) appears only in the lowest field ring resonance (and in N-H). Coupling through several bonds would appear more likely to affect H_{22} (four bonds away) than H_{24} (five bonds away through a nitrogen atom), but no firm basis exists for a final choice between the two possible assignments.

Exchange of the pyrrole N-H proton for deuterium should have the same effect as decoupling the N-H proton and, as a consistency check, this method was used for a comparison of the calcium complex with the free acid. It was apparent from inspection of Figures 2b and 3b (and confirmed by spin-decoupling the pyrrole N-H at 270 MHz in the calcium complex; spectrum not shown) that the coupling patterns of the three resonances on proceeding from downfield to upfield remain intact, demonstrating that no resonance crossovers have occurred upon complexation. Thus, the pyrrole proton (H_{22} or H_{24}) at 7.05 ppm moves 0.56 ppm downfield when calcium is added to A23187.

The benzoxazole N-H proton at 8.09 ppm in the free acid showed a tendency toward exchange on standing in chloroform solution, presumably with traces of ambient moisture. The upfield N-$C_{3'}$ methyl doublet was decoupled in these instances, thus confirming the N-H peak assignments. Since the carboxylic acid OH proton did not appear in any spectra obtained in this investigation (probably due also to exchange-broadening phenomena), it may be suggested that both the OH and benzoxazole NH protons are involved somewhat interchangeably in a hydrogen-bonded network linking the two nitrogen atoms in the benzoxazole portion of A23187 free acid.

Both NH resonances respond to the addition of calcium. The benzoxazole NH moves downfield ca. 1.2 ppm upon complexation, while the pyrrole NH travels downfield greater than 4 ppm to a very low field position at 13.97 ppm. (A similar position was observed for this proton in the magnesium complex of A23187 under the same experimental conditions.) Spectra of mixtures of acid and complex at various ratios in chloroform solution revealed separate, rather than averaged, resonances for both NH protons. This phenomenon, due to a spectral process which is "slow" on the NMR time scale (Bovey, 1969), is discussed further below.

Table I: Comparison of Proton Spin–Lattice Relaxation Values (T_1's) for A23187 Free Acid and Calcium Complex in Chloroform Solution.

A23187 Proton[a]	T_1, Free Acid (sec)[b]	T_1, Ca^{2+} complex (sec)[b]
H_4	0.94, 0.94[c]	0.52, 0.47[c]
H_5	1.48, 1.43[c]	0.80, 0.81[c]
H_{10}	0.52	0.23
H_{22} (or H_{24})[d]	1.21	0.63
H_{24} (or H_{22})[e]	1.05	0.47
H_{23}	1.36	0.82
$H_{3'}$ (N-CH_3)	0.53, 0.52[c]	0.33, 0.35[c]

[a] See Figure 1 for numbering system and Figure 5 for assignment of H_{10}. [b] Estimated uncertainty in experimental T_1 values: ±0.05 sec. [c] Resonances were doublets; T_1's obtained for each line of the doublet. [d] T_1 for resonance at 7.05 ppm. [e] T_1 for resonance at 6.92 ppm.

Proton Relaxation Measurements on A23187. The 2:1 A23187/Ca^{2+} stoichiometry of the complex—determined previously by atomic absorption (Pfeiffer et al., 1974) and other spectroscopic methods (Puskin and Gunter, 1975)—is supported by a preliminary set of proton spin–lattice relaxation data (T_1's). If the complex is a dimer (vs. the free acid) tumbling as an entity in solution, one may expect, in the absence of complicating factors, the values of T_1 obtained for the free acid monomer to drop by about a factor of two for the corresponding protons of the complex dimer (Doddrell et al., 1972; Richards and Sharp, 1975).

Samples of ca. 15 mg/ml of free acid and complex in chloroform solution were prepared by dissolving the A23187, bubbling dry nitrogen through the solution for 2 or 3 min, and then transferring to NMR tubes. (This method did not, however, exclude the presence of ambient oxygen.) T_1's were recorded at 90 MHz, using a $180°$-τ-$90°$-$5T_1$ sequence (Vold et al., 1968). Values of τ were varied at regular intervals between 0.05 and 1.60 sec. Data were processed using a nonlinear least-squares fit to each set of experimentally obtained peak heights. Only those individual A23187 resonances which were cleanly resolved at 90 MHz were useful in these experiments. Typical T_1 values for free acid and calcium complex are presented in Table I, where the trend of significantly lower T_1's for the complex (attributable to its higher molecular weight and, hence, longer rotational correlation time) is consistent with its presumed dimeric nature. No attempt was made to interpret the absolute values of T_1's in terms of molecular dynamics. The lower values of T_1 observed for the upfield half of the benzoxazole quartet (resonance at 6.65 ppm) vs. the downfield half (at 7.59 ppm) support the assignment of the 6.65-ppm peak to H_4, since its proximity to both an N-H and three *N*-methyl protons could facilitate its relaxation (vs. H_5). However, similar arguments based on numbers of proximal protons do not appear to clarify the assignments of the three pyrrole protons.

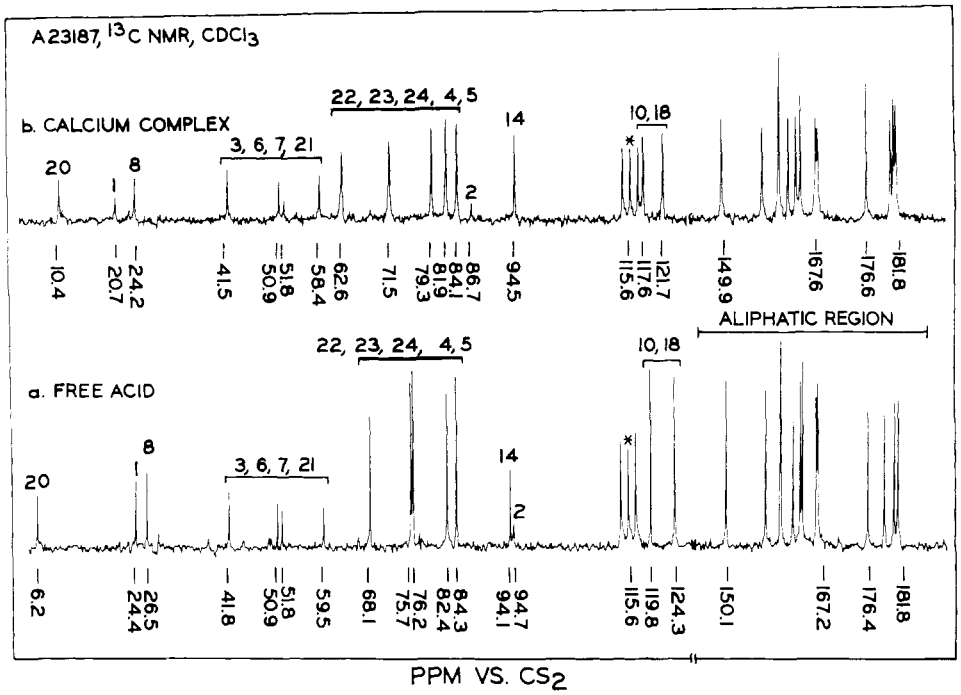

FIGURE 4: Carbon-13 NMR spectra (22.63 MHz) of A23187; concentration, 40–50 mg/ml in $CDCl_3$. Spectra are the result of ca. 50000 accumulations at a recycle time of 1.2 sec. Chemical shifts given in parts per million upfield from external carbon disulfide (CS_2) with $CDCl_3$ triplet (center peak marked with an asterisk) at 115.6 ppm. To convert to parts per million vs. internal Me_4Si, subtract the values given from 192.5 ppm. Spectra are: (a) free acid and (b) calcium complex. Omitted from the figure for clarity are the following additional groups of assignments in the aliphatic region: resonances between 150.1 and 167.2 (inclusive) in (a) and those between 149.9 and 167.6 in (b) represent carbons 9, 11, 12, 13, 15, 16, 17, 19, and 3′; resonances between 176.4 and 181.8 in (a) and those between 176.6 and 181.8 in (b) represent carbons 11′, 15′, 17′, and 19′ of A23187.

Carbon-13 NMR Spectra. Carbon-13 spectra of A23187 free acid and calcium complex, at 22.63 MHz, were compared under similar conditions of solvent, concentration, and spectral parameters (Figure 4). Resonances were assigned to groups of chemically similar carbons or to individual carbons where possible, using mainly empirical correlations with model compounds and resonance positions of common functional groups. Through the study of proton undecoupled spectra, carbons directly bound to protons were readily identified through their splitting due to direct ^{13}C–^{1}H coupling (ca. 150 Hz). The apparent reduced peak intensity of several resonances in Figure 4 is attributable to the fact that they are only partially relaxed at the 1.2-sec recycle time employed. This result, taken together with the relatively sharp appearance of these latter resonances even in undecoupled spectra, indicates that they correspond to unprotonated (quaternary) carbon atoms.

Although there are only two carbonyl carbons in the molecule (C_1 and C_{20}), three resonances appear in the "carbonyl region" (at 6.2, 24.4, and 26.5 ppm). The odd resonance is believed to be the carbon located between the N and O atoms in the benzoxazole ring (C_8); proximity to these electronegative atoms, in addition to both its aromatic and quaternary character, could produce a low-field position for this atom. The ^{13}C spectrum of the model compound 2-methylbenzoxazole in chloroform solution contains a resonance in this region (at 29.0 ppm) which may be ascribed to the corresponding quaternary carbon atom (C_2) in the model compound. Assignments of carbonyls shown in Figure 4 are again based on the spectral regions typically found for each type. The choice between C_1 and C_8 was made from the undecoupled spectra in which the resonance assigned to C_1 remained sharp. This carbon is the most distant of the three from nonexchangeable protons, and hence the least coupled.

While the methyl and methylene resonances remain relatively unchanged (one methyl resonance moves about 1.5 ppm, the only significant change in the aliphatic region; see Figure 4), comparison of the downfield regions of the free vs. complexed spectra reveals large chemical-shift changes in several instances. In order to determine precisely which resonances in the free acid correspond to those in the calcium complex, advantage was taken of the observation from proton spectra that a slow exchange process existed at probe temperature between the two forms of A23187. Thus, the ^{13}C spectrum of a ca. 50:50 mixture (by weight) of the free acid–calcium complex, total concentration ca. 80 mg/ml in $CDCl_3$, was recorded and analyzed. In such an experiment, three possibilities arise: (i) those carbons whose chemical shifts differ significantly between the free and complexed states should present broadened resonances in various stages of coalescence; (ii) those carbons whose shifts are nearly the same in both states should appear as single sharp lines; and (iii) those whose shifts in the two states are so widely different that coalescence at probe temperature has not begun should appear as pairs of fairly sharp lines. With respect to condition iii, it was already known from studies of the N–H regions at 90 MHz in proton spectra that resonances separated by at least 100 Hz—which would correspond to about 5 ppm in the present carbon spectra—have not yet begun to coalesce at 30°. The results from these coalescence experiments demonstrated that several resonances experienced changes of 1.5 ppm or greater upon complex formation; these were found to be paired as follows (free acid chemical shift, chemical shift for same carbons in complex): (6.2, 10.4), (24.4, 20.7), (26.5, 24.2), (68.1, 62.6), (75.7 and 76.2, 71.5 and 79.3), (119.8, 117.6), (124.3, 121.7), and (179.4, 180.9). One important result from these

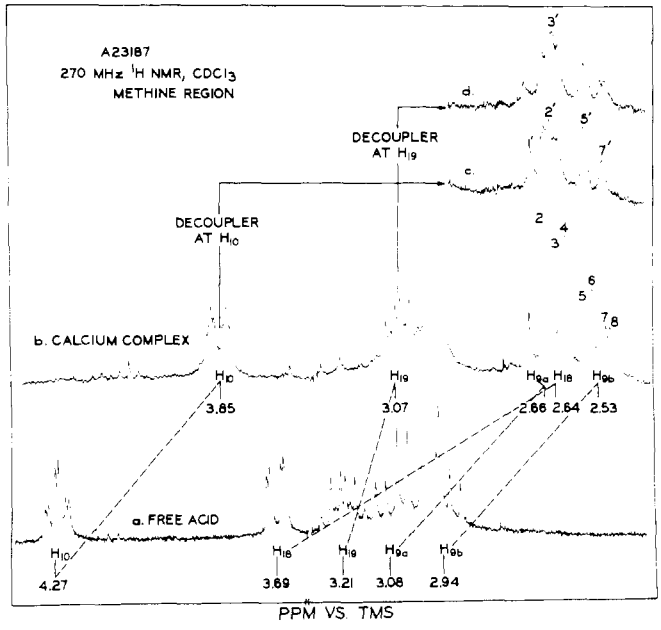

FIGURE 5: Proton NMR spectra (270 MHz) of a portion of the methine region of A23187; concentration, 5 mg/ml in $CDCl_3$. Chemical shifts given in parts per million vs. internal Me_4Si. Assignments to particular protons and their individual chemical shifts are indicated. Spectra are: (a) free acid; (b) calcium complex; (c) same as (b) but with homonuclear spin decoupling at 3.85 ppm; (d) same as (b) but with decoupling at 3.07 ppm. Dashed lines show the movements of various protons upon complexation. Truncated resonances in (a) and (b) near 3.0 ppm correspond to the 3'-*N*-methyl group. For further comments on the figure, see text.

data is that all three resonances in the carbonyl region experience major chemical-shift changes (2–4 ppm) upon addition of calcium.

Although it was confirmed that three of the five resonances between 68.1 and 84.3 in spectrum 4a undergo chemical-shift changes of 3–5 ppm upon addition of calcium, it remains to be determined precisely which two of the five correspond to the benzoxazole protonated carbons (C_4 and C_5), and which three to pyrrole ring protonated carbons (C_{22}, C_{23}, and C_{24}). Comparisons with ^{13}C spectra of model compounds are of interest; 2-methylbenzoxazole contains four protonated carbons which resonate at 68.4, 68.7, 73.4, and 82.6 ppm, while pyrrole-2-carboxaldehyde contains three protonated carbons which resonate at 65.3, 70.5, and 81.7. However, these results, combined with the substituent effects certain to influence A23187 chemical shifts, do not produce unequivocal assignments. It is certain, however, that at least one pyrrole carbon resonance changes its chemical shift significantly.

Using line widths determined experimentally from ^{13}C spectra, estimates of the rotational correlation times of the free acid and complex in solution could be made. Line widths of the free acid (3.0 ± 0.5 Hz) increased in the calcium complex to 5.5 ± 0.5 Hz. Using the relationship that the line width at half-height is equal to $1/\pi T_2$ (Bovey, 1969), one obtains values of T_2 = 0.11 sec for the free acid and T_2 = 0.06 sec for the complex. From plots of the dependence of T_2 on rotational correlation time presented by Doddrell et al. (1972), values of 0.3 nsec for the free acid and 0.8 nsec for the calcium complex are obtained. Case et al. (1974) reported values of <2 nsec for the acid and 11 nsec for the complex embedded in mitochondrial membranes, while Puskin and Gunter (1975) obtained a value of 1–2 nsec for the calcium complex in sonicated egg lecithin. The present results, recorded in the medium of highest fluidity of the three—chloroform solution—are consistent with the expectation of increased molecular mobility and hence shortest rotational correlation times. In general, results from the ^{13}C line-width measurements also support the 2/1 A23187/Ca^{2+} stoichiometry determined from proton T_1 measurements.

The free energy of activation $\Delta G^{\ddagger}$ for exchange between free and complexed A23187 molecules was estimated from the knowledge that a separation of ca. 1.7 ppm (= 38 Hz in the present ^{13}C spectra) at 30° would give rise to a resonance which was judged to be at coalescence. Using the formulation of Shan-Atidi and Bar-Eli (1970) and assuming equal populations of the two states, $\Delta G^{\ddagger}$ = ca. 15.0 kcal/mol for this process. Although the stepwise mechanism for ionophore exchange has not been elucidated, this barrier likely corresponds to the exchange of a free acid A23187 molecule with one (of the two) anionic A23187 molecules comprising the calcium complex.

Geometry of the A23187 "Hinge" Regions. A more detailed conformational analysis was now essential to ascertain specific geometric features of the two forms of A23187. Our approach to this problem involved the measurement of vicinal coupling constants between protons in critical portions of the A23187 molecule, followed by analysis of the values thus obtained using a Karplus-type relationship (Karplus, 1959, 1963; Bystrov et al., 1973). By this method, values of backbone rotational dihedral angles consistent with NMR spectra may be extracted, and in conjunction with model building studies, reasonable conformations can be suggested.

For the purposes of conformational analysis, the A23187 molecule may be divided into three portions: the spiroketal backbone (consisting of the two aliphatic-rich six-membered rings); the benzoxazole ring; and the pyrrole ring. Upfield regions of proton spectra (including most of the backbone methyl and methylene protons) were highly complex and provided no direct conformational information; geometry in this portion of the molecule was determined largely by assuming an axial-axial spiroketal linkage (Chaney et al., 1974). Spectral results already described indicate little change upon complexation in this region of the molecule; for example, compare the aliphatic regions of ^{13}C spectra of free and complexed forms (Figure 4, a and b). Additional limitations on allowed conformations of A23187 are imposed by the conjugated—and hence, planar—nature of the two aromatic moieties and their substituents (i.e., the atoms between C_1 and C_8, and those between C_{20} and C_{24}). However, considerable free rotation is possible in the regions where this backbone is joined to each of the aromatic rings (the "hinge" regions), particularly about C_9–C_{10} and C_{18}–C_{19} single bonds. We have used 270-MHz proton NMR spectra to determine molecular geometry in these regions.

Spectra of the methine regions of free and complexed A23187, shown in Figure 5, proved especially informative. Several individual protons of the hinge regions are resolved and an analysis of coupling constants could be carried out. Proton assignments were made on the basis of chemical shifts, coupling patterns, and, in the calcium complex, through the application of homonuclear spin decoupling. The benzoxazole hinge region contains the C_9 methylene group, with protons H_{9a} and H_{9b} coupled to each other (with a large geminal coupling) and to H_{10}. The latter pro-

Table II: Coupling Constants and Dihedral Angles in the Hinge Regions of A23187.[a]

Protons $i-j$	Coupling Constant, $J_{H_i-H_j}$ (Hz)		Dihedral Angles,[b] $H_i-C-C-H_j$ (deg)	
	Free Acid	Calcium Complex	Free Acid	Calcium Complex
9a–9b	15.2[c]	13.3[c]		
9a–10	7.3	11.2	150	180
9b–10	7.5	3.0	30	60
10–11	2.4	1.8	~90	~90
17–18	2.0	<2.0	~90	~90
18–19	10.1	10.1	180	180
19–19′	6.8	6.8	*d*	*d*

[a] Coupling constants determined from 270-MHz proton spectra in deuteriochloroform solution. Protons numbered according to scheme given in Figure 1. Protons 9a,b, 10, and 11 are in the benzoxazole hinge region; protons 17, 18, 19, and 19′ are in the pyrrole region. [b] Dihedral angles deduced from Karplus-type relationship; estimated uncertainty, ±15°. [c] Geminal coupling constant (all others vicinal). [d] Measured coupling constant reflects average of rotamers of three $H_{19'}$ protons.

ton is further coupled to H_{11} (not shown in Figure 5). In the pyrrole hinge region, H_{18} and H_{19} are resolved.

The pattern of overlapping resonances between 2.5 and 2.7 ppm in the complex (Figure 5b) was clarified through spin decoupling. When the decoupler was placed at H_{10} in Figure 5b, coupling was eliminated between this proton and H_{9a} and H_{9b}. This coupling, which gives rise to lines numbered 1, 2, 4, 5, 6, 7, and 8 in Figure 5b, collapses to the AB quartet of lines due to geminal $H_{9a}-H_{9b}$ coupling, numbered 1′, 2′, 5′, and 7′ in Figure 5c. (Note that line 1′ is actually about 5 Hz upfield of line 1.) Similarly, when the calcium spectrum was decoupled at H_{19}, the resulting pattern (Figure 5d) revealed that coupling between H_{9a}, H_{9b}, and H_{10} remained intact, but that lines numbered 3 and 4 in Figure 5b (representing the large coupling between H_{18} and H_{19}) were collapsed to a broad resonance (numbered 3′ in Figure 5d).

Vicinal coupling constants between the various protons are summarized in Table II along with calculated dihedral rotational angles. Significantly, constants in the pyrrole hinge region are unchanged upon complexation, suggesting little or no geometric change in the C_{17} to C_{19} portion of the molecule. However, coupling constants (and hence dihedral angles) between H_{9a}, H_{9b}, and H_{10} change considerably when calcium is added, indicating conformational alteration in the benzoxazole hinge portion of the A23187 molecule.

Discussion

Conformation of the A23187 Free Acid and Complexed Anion in Solution. The NMR results obtained herein allow the specification, within a relatively narrow range, of the probable conformations of the A23187 free acid dissolved in chloroform solution and of the corresponding A23187 anion which comprises half of the dimeric calcium complex. Considerations discussed in the Results section, based on the structural rigidity of the spiroketal linkage, the planarity of two conjugated aromatic moieties, and the limitations of dihedral angles imposed in the hinge regions resulting from the Karplus-type analysis, lead directly to the solution structures depicted in Figures 6a and 6b. The portion of the

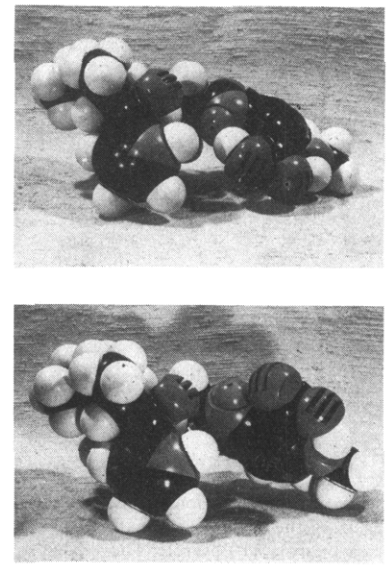

FIGURE 6: Photographs of Corey–Pauling–Koltun (CPK) space-filling models of (a, top) the conformation deduced for A23187 as the free acid in chloroform solution compared with (b, bottom) the conformation deduced for one of the two (equivalent) A23187 anions which comprise the calcium complex. Note the comparative relationship of the potential liganding atoms (the pyrrole oxygen [left, grooved], the benzoxazole nitrogen [center, gray capped], and one carboxylate oxygen [grooved, nearer to capped nitrogen, protonated in (a)]). In the complex conformation (b), these atoms are proximal and appropriately oriented to form a portion of a metal binding site. The proton visible just behind the pyrrole oxygen (top, center of model) in both (a) and (b) is H_{9b}.

A23187 molecule containing all the atoms between C_{10} and C_{19} inclusive has essentially the same geometry in both forms.

The most significant change found by NMR studies between the free acid and the complex (aside from the presumed monomeric and protonated nature of the acid) is in the dihedral angle about the C_9-C_{10} single bond. Coupling data clearly indicate a 20–40° change in this angle; models suggest that when this angular rotation is made, the benzoxazole ring actually swings away from the pyrrole region. If this occurs, the intramolecular H-bond between the pyrrole NH and the benzoxazole carboxylic acid group found by x-ray analysis in the solid state (Chaney et al., 1974) for the free acid—and which may persist in chloroform solution—would probably not be present in the complexed A23187 anion. (However, see discussion below concerning *intermolecular* H bonding in the calcium complex.)

NMR data provide no direct information on the rotational states of the $C_{19}-C_{20}$ and C_8-C_9 single bonds. Once the molecule is placed in the conformation deduced for the free acid, models indicate that, despite intramolecular steric interactions, an arc of rotation of at least 60° is possible for the α-ketopyrrole group about the $C_{19}-C_{20}$ single bond. Although it appears at first that free rotation of the benzoxazole group should be possible around the C_8-C_9 single bond, the $C_{11'}$ methyl group partially hinders attempts to rotate this ring in the free acid conformation. Not only is this hindrance removed in the calcium complex (after the prescribed change in the C_9-C_{10} dihedral angle), but it may be seen that the C_9-methylene group acts as a buffer zone, in that the separation in space between the benzoxazole liganding sites and the pyrrole keto group is regulated by the rotational state about the C_9-C_{10} bond.

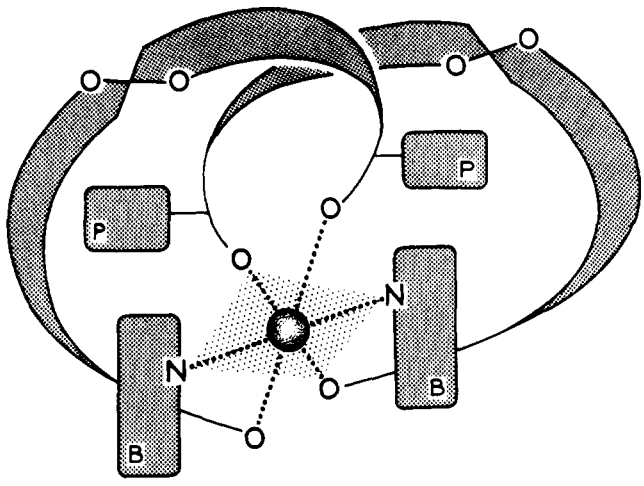

FIGURE 7: Schematic representation of the proposed A23187–calcium complex, emphasizing the pseudocyclic nature of each folded A23187 molecule: (B) benzoxazole; (P) pyrrole. The shaded square around the central cation indicates the square planar arrangement of the ligands. Hydrogen bonding interactions have been omitted.

Conformation of the Calcium Complex of A23187 in Solution. Several key aspects of the experimentally obtained spectral data, as well as model-building studies, were used as input in the construction of the proposed solution structure of the A23187 calcium complex. We believe it is logical to assume that one of the benzoxazole carboxylate oxygen atoms participates in calcium binding since: (i) the preparation of the complex appears to involve the direct exchange between nonpolar and aqueous media of $2H^+$ for Ca^{2+}; (ii) the methyl ester analog of A23187 complexes with divalent cations orders of magnitude more weakly than A23187 itself under comparable conditions (D. R. Pfeiffer, this laboratory, unpublished results); and (iii) the greatest component of A23187–metal ion interaction has been shown to be "ionic" (Puskin and Gunter, 1975). Both proton and ^{13}C NMR spectra have indicated involvement also of the pyrrole moiety in binding, presumably through its α-keto function. Furthermore, in view of the dimeric nature of the complex, the observation of only one set of resonances for two A23187 molecules suggests that the complex has a form of C_2 symmetry in which both molecules have identical magnetic environments and conformations (although some rapid local conformational averaging in the two molecules of $Ca(A23187)_2$ would be undetected at probe temperature in NMR spectra).

Finally, as indicated above, the set of dihedral angles obtained through the analysis presented in Figure 5 and Table II drastically narrows the possible conformations, especially in the important hinge regions.

Even if it is assumed that individual complexed A23187 anions take up the conformation determined above, the NMR data cannot specify precisely (as does x-ray analysis) how two A23187 anions should be brought into proximity. Thus, it should be emphasized that considerations from model-building studies play an important role in this phase of the investigation. Furthermore, since a solution conformation represents a dynamic rather than a static situation, a continuum of states is likely, i.e., at any instant, the two A23187 molecules may be slightly closer or further apart, or a specific hydrogen bond may dissociate and form again to a neighboring ligand. This notion is emphasized here to counter the tendency to view a conformation deduced in solution (and constructed from molecular models) as a fixed conformation.

One structure consistent with available data, using the conformation deduced for the A23187 anion, is presented in schematic form in Figure 7. Individual A23187 anions take up a folded, pseudocyclic conformation (which may be compared to an "unclosed ellipse") surrounding the calcium atom. In addition, the two (identical) A23187 molecules have been brought together and wrapped around each other. This structure contains a central binding site with an array of four benzoxazole and pyrrole carbonyl oxygen atoms, while the calcium atom is appropriately positioned to interact as well with the aromatic nitrogen atom (between C_7 and C_8) of each benzoxazole ring. Stereochemically, this bonding situation may be described as a slightly distorted octahedral coordination to calcium. Puskin and Gunter (1975) have similarly proposed a distorted octahedral arrangement of liganding groups, based on electron paramagnetic resonance (EPR) observations of the Mn^{2+} complex of A23187.

Models suggested that the spiroketal oxygen atoms in A23187 were relatively inaccessible for binding, due to local steric interactions with surrounding aliphatic groups, and were comparatively distant from the calcium ion when other likely liganding sites were situated in close proximity to it. However, coordination to ether oxygens occurs widely in numerous ionophores (e.g., of the nigericin, monensin, X-537A types, etc.) (Ovchinnikov et al., 1974) and the possible involvement of (at least one of) the spiroketal oxygens in binding was therefore considered. In contrast to the A23187 structure, many ether oxygen atoms in other ionophores are found as parts of tetrahydrofuran rings (or as hydroxyl groups) which may allow for their closer approach to cations than is possible for ethers locked into a spiro linkage. Backbone rotational freedom is generally greater as well in other ionophores, thus imparting more flexibility in ligand arrays. Further, the observed selectivity of A23187 for divalent cations vs. monovalents does suggest some variation from the usual categories of ligands (e.g., greater importance of the aromatic conjugated carbonyl ligands). Nevertheless, upon calcium binding, chemical-shift changes occur in the carbon resonances on either side of the A23187 spiro oxygens (C_{10} and C_{18}), as well as in corresponding proton resonances (H_{10} and H_{18}). While it may be tempting to ascribe these changes to the binding of calcium to adjacent ether linkages, several other factors may be cited which can also account for the observed chemical-shift changes. In the deduced structures, for example, the keto group of the pyrrole portion of the molecule is oriented directly toward H_{10} and H_{18}, such that rotations about the C_{19}–C_{20} bond (which probably occur upon complex formation) will alter the spatial relationships between these two protons and the anisotropic ketopyrrole π system. In addition, the C_{10}–H and C_{18}–H bonds are directed toward the binding cavity; when the doubly positive cation is introduced, proximity to the positive sphere of charge will not only influence local magnetic environments, but could result in an inductively induced polarization of these C–H bonds. In a discussion of the NMR spectra of the ionophore nonactin and its potassium complex, where ion binding is believed to involve primarily carbonyl oxygens, Prestegard and Chan (1969) have similarly suggested ion-induced polarization of neighboring C–H bonds as the origin of chemical-shift changes which occur in the vicinity of nonactin (tetrahydrofuran) ether oxygens. Such polarization could

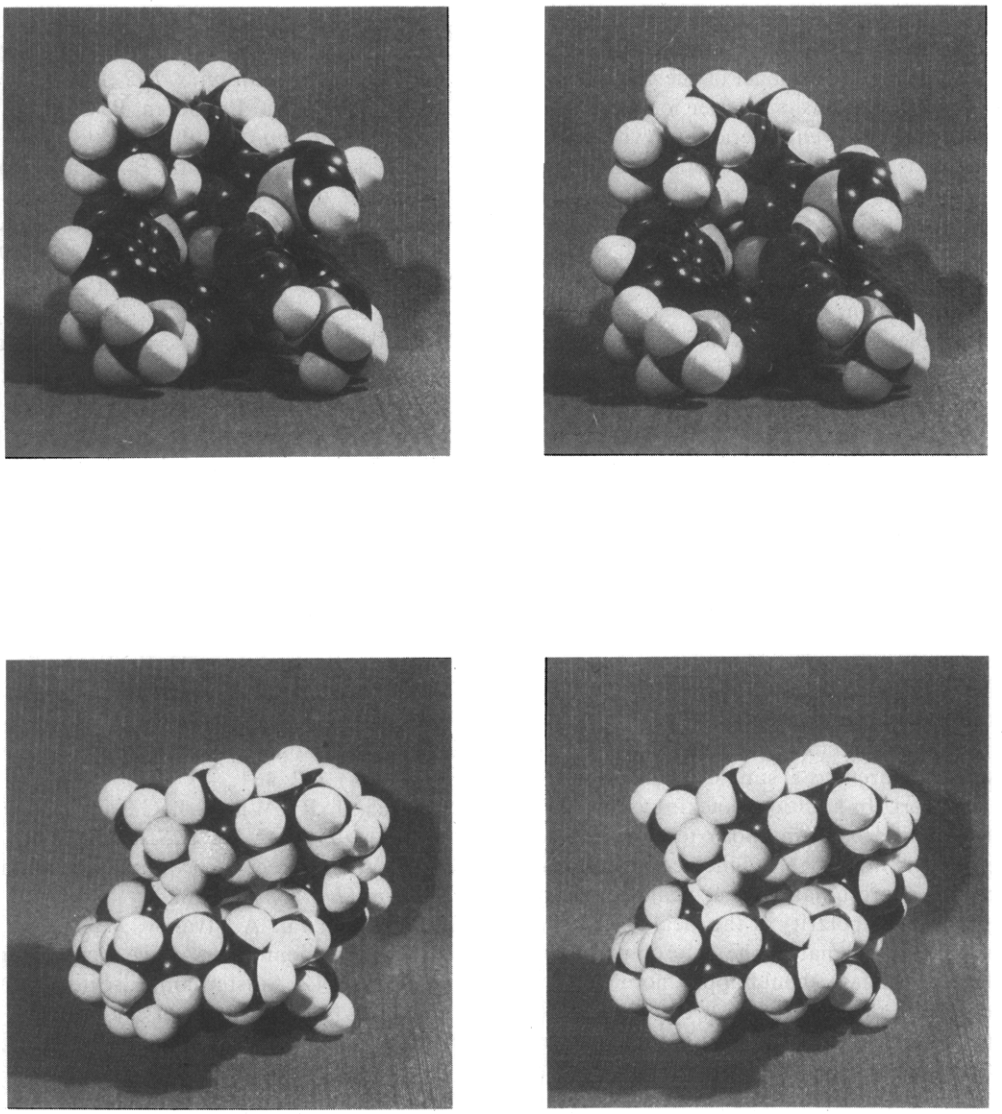

FIGURE 8: Stereophotographs of the conformation proposed for the A23187–calcium complex in solution, using CPK space-filling models. In view a (top), the central binding site and metal atom may be observed. In view b (bottom), the model has been rotated about 180° to illustrate the shielding of the cation provided by the aliphatic backbones of the two A23187 molecules.

explain the experimental observations in the present work that chemical-shift changes occur in opposing directions for directly bonded atoms (i.e., C_{10} downfield, H_{10} upfield). Thus, whether or not either of the A23187 spiroether oxygen atoms actually participates in cation binding, the data herein do suggest significant electronic perturbations upon complex formation in the vicinity of these atoms.

Because of the particularly low-field position of the pyrrole NH proton in the complex (13.97 ppm), one is led to suggest that a further stabilizing interaction may be present. Upon reorganization of electron density in the pyrrole ring—as negative charge flows toward the conjugated carbonyl group (C_{20}=O) for its participation in binding—the pyrrole ring nitrogen atom acquires residual positive charge. Hence, the pyrrole NH proton itself becomes partially positive and is thus deshielded. Simple proximity to the double positive charge of the metal cation may also contribute to deshielding. However, after the ligands are positioned in the model as already described, the pyrrole NH can form an intermolecular N–H···O (or perhaps N–H···N) bridge to the benzoxazole carboxylate group (or aromatic nitrogen atom) of the other A23187 molecule. Such hydrogen bonding might then shift this proton further downfield to the spectral region observed. Although the analogy is obviously not precise, the low-field position of the pyrrole proton, and its possible involvement in a hydrogen bridge between two aromatic heterocycles, recalls the base pairing of transfer RNA, in which comparable low-field positions are observed for protons so involved (Kearns et al., 1973). In the proposed A23187 conformation, however, the two aromatic moieties are not close to coplanarity nor oriented as they are in tRNA and any such hydrogen bond may be of only moderate strength.

Stereophotographs of two views of Corey–Pauling–Koltun (CPK) space-filling models of the proposed solution conformation of A23187–calcium complex are presented in Figure 8. Largely on the basis of model-building considerations, the structure shown was chosen in preference to the geometric isomer in which one A23187 molecule is rotated ca. 180° (about an axis through C_{14} and bisecting the O–C–O linkage) and then rejoined to its unchanged counterpart. This operation, which juxtaposes the two benzoxazole and two pyrrole moieties, appears to eliminate the possibility of hydrogen-bond bridging, and creates several un-

favorable steric contacts between polar and nonpolar groups at points of close approach between the two molecules.

The proposed conformational model of the calcium complex is analogous to other diffusion carrier ionophores, i.e., the cation is shielded from solvent interactions while the exterior of the complex is highly hydrophobic so as to impart lipid solubility. However, A23187 apparently forms other types of complexes with Cu^{2+} (Puskin and Gunter, 1975) and La^{3+} and monovalent cations (Pfeiffer et al., 1974) in which the degree of similarity to the Ca^{2+} structure proposed here is not yet known. It is of particular importance to elucidate further the chemical basis and extent of selectivity of A23187 for divalent over monovalent cation transport, especially since this selectivity constitutes the principal utility of the compound. From the present results, we can suggest that cation charge selectivity for transport may arise in part from ineffective shielding of the cation from solvent in monovalent cation complexes of 1:1 stoichiometry and/or from a requirement for a high charge-to-radius ratio in the cation due to the involvement of the electron-rich aromatic moieties in binding. Until more definitive data are available, the possibility of monovalent cation transport by A23187 under some conditions should not be ignored.

In terms of the detailed mechanism of transport, the substantial barrier to interconversion between A23187 and its Ca^{2+} complex observed herein argues against a carrier-relay mechanism, compared to a simple diffusion mechanism of cation transport. In addition, stacking of the molecules (using the deduced conformation) to form ion-conducting channels seems improbable. Since complexing and decomplexing reactions presumably occur near membrane–water interfaces where the polarity of the local environment would be much higher than that of the chloroform used in these studies, the present data should apply more closely to the conformation of the molecule when it traverses the hydrophobic interior of the membrane. Thus, the conformational differences between free acid and complex reported here may not relate precisely to those changes occurring during the overall process of cation transport. Nevertheless, folding and unfolding of A23187 similar to that observed herein on passing from complex to free acid could in principle (a) facilitate the requisite cation–proton interchanges at membrane surfaces by exposing the carboxylate group to the aqueous medium, as well as (b) enhance the rate of cation complexing (and decomplexing) reactions by allowing stepwise substitution of A23187 ligands for solvent molecules.

Acknowledgments

The authors are grateful to Professor Henry A. Lardy for his enthusiasm and support throughout the course of this work. We thank Mr. James Blackbourn (Pharmacy) and Dr. David Hillenbrand (Chemistry) for their assistance in recording NMR spectra. Helpful discussions with Dr. Michael Chaney of Eli Lilly and Co. are also gratefully acknowledged.

References

Arlinger, L., Dahlqvist, K.-I., and Forsen, S. (1970), *Acta Chem. Scand. 24,* 672.

Bovey, F. A. (1969), in Nuclear Magnetic Resonance Spectroscopy, New York, N.Y., Academic Press, pp 183–210.

Bystrov, V. F., Portnova, S. L., Balashova, T. A., Koz'min, S. A., Gavrilov, Yu. D., and Afanas'ev, V. A. (1973), *Pure Appl. Chem. 36,* 19.

Case, G. D., Vanderkooi, J. M., and Scarpa, A. (1974), *Arch. Biochem. Biophys. 162,* 174.

Caswell, A. H., and Pressman, B. C. (1972), *Biochem. Biophys. Res. Commun. 49,* 292.

Chambers, E. L., Pressman, B. C., and Rose, B. (1974), *J. Cell Biol. 63,* 56a.

Chaney, M. O., Demarco, P. V., Jones, N. D., and Occolowitz, J. L. (1974), *J. Am. Chem. Soc. 96,* 1932.

Deber, C. M., and Blout, E. R. (1974), *J. Am. Chem. Soc. 96,* 7566.

Doddrell, D., Glushko, V., and Allerhand, A. (1972), *J. Chem. Phys. 56,* 3683.

Eisenman, G., and Krasne, S. J. (1973), *MTP Int. Rev. Sci., Biochem. Ser. One 2,* 1–33.

Foreman, J. C., Mangar, J. L., and Gomperts, B. D. (1973), *Nature (London) 245,* 249.

Grenier, G., Van Sande, J., Glick, D., and Dumont, J. E. (1974), *FEBS Lett. 49,* 96.

Holz, R. (1975), *Biochim. Biophys. Acta 375,* 138.

Karplus, M. (1959), *J. Chem. Phys. 30,* 11.

Karplus, M. (1963), *J. Am. Chem. Soc. 85,* 2875.

Kearns, D. R., Lightfoot, D. R., Wong, K. L., Wong, Y. P., Reed, B. R., Cary, L., and Shulman, R. G. (1973), *Ann. N.Y. Acad. Sci. 222,* 324.

Levy, J. V., Cohen, J. A., and Inesi, G. (1973), *Nature (London) 242,* 461.

Luckasen, J. R., White, J. G., and Kersey, J. H. (1974), *Proc. Natl. Acad. Sci. U.S.A. 71,* 5088.

Maino, V. C., Green, N. M., and Crumpton, M. J. (1974), *Nature (London) 251,* 324.

Ovchinnikov, Yu. A., Ivanov, V. T., and Shkrob, A. M. (1974), in Membrane-Active Complexones, B. B. A. Library Vol. 12, Amsterdam, Elsevier, pp 111–209.

Patel, D. J. (1973), *Biochemistry 12,* 677.

Pfeiffer, D. R., Reed, P. W., and Lardy, H. A. (1974), *Biochemistry 13,* 4007.

Prestegard, J. H., and Chan, S. I. (1969), *Biochemistry 8,* 3921.

Prince, W. T., Rasmussen, H., and Berridge, M. J. (1973), *Biochim. Biophys. Acta 329,* 98.

Puskin, J. S., and Gunter, T. E. (1975), *Biochemistry 14,* 187.

Reed, P. W., and Lardy, H. A. (1972a), *J. Biol. Chem. 247,* 6970.

Reed, P. W., and Lardy, H. A. (1972b), in The Role of Membranes in Metabolic Regulation, Mehlman, M. A., and Hanson, R. W., Ed., New York, N.Y., Academic Press, pp 111–131.

Reed, P. W., Pfeiffer, D. R., and Lardy, H. A. (1975), in Proceedings of the Second Annual New England Bioengineering Conference, Peura, R. A., et al., Ed., Burlington, Vt., Vermont University Press, pp 73–80.

Richards, E. P., and Sharp, R. R. (1975), *Biochem. Biophys. Res. Commun. 64,* 851.

Schaffer, S. W., Safer, B., Scarpa, A., and Williamson, J. R. (1974), *Biochem. Pharmacol. 23,* 1609.

Schroeder, T. E., and Strickland, D. L. (1974), *Exp. Cell Res. 83,* 139.

Schwartz, A., Lewis, R. M., Hanley, H. G., Munson, R. G., Dial, F. S., and Ray, M. V. (1974), *Circ. Res. 34,* 102.

Selinger, Z., Eimerl, S., and Schramm, M. (1974), *Proc. Natl. Acad. Sci. U.S.A. 71,* 128.

Shan-Atidi, H., and Bar-Eli, K. H. (1970), *J. Phys. Chem. 74,* 961.

Simon, W., Morf, W. E., and Meier, P. Ch. (1973), *Struct. Bonding (Berlin) 16,* 113.
Steinhardt, R. A., and Epel, D. (1974), *Proc. Natl. Acad. Sci. U.S.A. 71,* 1915.
Steinhardt, R. A., Epel, D., Carrol, E. J., and Yanagamachi, R. (1974), *Nature (London) 252,* 41.
Thoa, N. B., Costa, J. L., Moss, J., and Kopin, I. J. (1974), *Life Sci. 14,* 1705.
Truter, M. R. (1973), *Struct. Bonding (Berlin) 16,* 71.
Vold, R. L., Waugh, J. S., Klein, M. P., and Phelps, D. E. (1968), *J. Chem. Phys. 48,* 3831.
Wollheim, C. B., Blondel, B., Trueheart, P. A., Renold, A. E., and Sharp, G. W. G. (1975), *J. Biol. Chem. 250,* 1354.
Wong, D. T., Wilkenson, J. R., Hamill, R. L., and Horng, J.-S. (1973), *Arch. Biochem. Biophys. 156,* 578.
Zahlten, R. N., Stratman, F. W., and Lardy, H. A. (1973), *Proc. Natl. Acad. Sci. U.S.A. 70,* 3213.

On the Free-Energy Changes in the Synthesis and Degradation of Nucleic Acids†

Leonard Peller

ABSTRACT: Standard free-energy changes for reactions involving single- and double-stranded nucleic acids have been related to that for polynucleotide synthesis from ribonucleoside diphosphates for which $\Delta G^{\circ\prime} \approx 0$. For polynucleotide formation from triphosphates this quantity is about -1 kcal. In the replication reaction the base pairing interactions are quantitatively of comparable importance. Production of a hydrolytic break in a double strand is substantially less favorable than in a single strand. The resealing of breaks utilizing ATP and NAD^+ have similar free-energy changes and are entropy driven processes. The highly exergonic hydrolysis of pyrophosphate is maintained to be of significance for both in vivo and in vitro polymerizations.

The free-energy changes accompanying enzyme-catalyzed synthetic and degradative reactions of nucleic acids have received little systematic experimental investigation. Nevertheless, the limited available data allow estimates to be made of these thermodynamic quantities for a number of important reactions. While the thermodynamics is of intrinsic interest, it is our view that considerations of this nature may be of greater significance in understanding these processes than has generally been assumed.

The results and analysis presented here are conveniently divided into two categories. Information in the first category concerns the thermodynamics of reactions involving single-stranded nucleic acids. These results when combined with thermodynamic data on the coil to helix transition provide estimates of companion quantities for reactions in the second category, double-stranded nucleic acids. Finally, the reactions involved in nucleic acid synthesis are examined in relation to the hydrolysis of the pyrophosphate by-product.

The reactions to be considered all involve phosphoric acids, esters, and anhydrides. It has long been recognized that such equilibria exhibit a marked dependence on pH and divalent metal ion concentration, e.g. Mg^{2+} (Podolsky and Sturtevant, 1955; Podolsky and Morales, 1956). We have adhered to the common practice of choosing a standard state of 1 *M* concentration of the total equilibrium distribution of ionic forms of each reactant species present at pH 7.0 with Mg^{2+} equal to 10^{-3} *M* and ionic strength of 0.15 at 25°C. As data are not always at hand for this state, we have occasionally been compelled to combine results obtained under somewhat different conditions. From this difficulty as well as from inherent experimental variations an uncertainty of ±1 kcal must attend all the primary results quoted below. However, even a wider incertitude would not seriously impair the main conclusions of this report as to the relative importance of the various contributions to the driving forces for the reactions of double-stranded nucleic acids.

Single-Stranded Nucleic Acids

Polynucleotide Synthesis from Nucleoside Diphosphates. The enzyme polynucleotide phosphorylase catalyzes the readily reversible reaction (a) depicted in Figure 1. The equilibrium constant for the addition of one nucleotide can be obtained in the manner first employed for the analogous primer initiated polysaccharide synthesis from glucose 1-phosphate with orthophosphate also the product (Trevelyan et al., 1952). With a given ribonucleoside diphosphate (rNDP) as reactant this quantity can be computed from the ratio of the equilibrium concentrations of orthophosphate to the unreacted monomer, i.e.

$$K_{1a} \approx [P]_{eq}/[rNDP]_{eq} = [P]_{eq}/\{[rNDP]_0 - [P]_{eq}\} \quad (1)$$

where $[rNDP]_0$ is the initial concentration of this latter species.

Some years ago this was shown to be tantamount to requiring that the probability (p) of propagation for the equilibrium most probable distribution where

$$p = ([rNDP]_{eq}/[P]_{eq})\, K_{1a} \quad (2)$$

approach unity (Peller, 1961; Peller and Barnett, 1962). This is the condition for achievement of high degrees of polymerization. Obviously the choice of values of p somewhat

† From the Cardiovascular Research Institute, University of California, San Francisco, California 94143. *Received September 2, 1975.* This work was supported by NHLI Grant No. HL-06285 and by the Samuel R. Neider Heart Research Fund.